Int. J. Adv. Appl. Math. and Mech. 3(1) (2015) 10 – 23 (ISSN: 2347-2529)

Journal homepage: www.ijaamm.com

IJAAMM

International Journal of Advances in Applied Mathematics and Mechanics

Numerical prediction of Taylor-Dean flow through a rotating curved duct with constant curvature

Research Article

Rabindra Nath Mondal[a, *], **Poly Rani Shaha**[a], **Nayan Kumar Poddar**[a], **Shinichiro Yanase**[b]

[a] *Department of Mathematics, Jagannath University, Dhaka-1100, Bangladesh*

[b] *Department of Mechanical and Systems Engineering, Faculty of Engineering, Okayama University, Okayama 700-8530, Japan*

Received 09 June 2015; accepted (in revised version) 17 August 2015

Abstract: In this paper, a spectral-based numerical study is presented for the fully developed two-dimensional flow of viscous incompressible fluid through a rotating curved duct with square and rectangular cross section. Numerical calculations are carried out for the Dean number, $Dn = 1000$, with positive rotation of the duct for the Taylor number $Tr = 100$, 500 and 1000 over the aspect ratios 1, 2 and 3. Spectral method is used as a basic tool to solve the system of non-linear partial differential equations. The main objective of the present study is to discuss the unsteady flow behavior i.e whether the unsteady flow is steady-state, periodic or chaotic, if Tr is increased. In order to investigate the non-linear behavior of the unsteady solutions, time evolution calculations of the unsteady solutions are performed and it is found that for the rotating square duct flow (aspect ratio 1) periodic flow turns into steady-state flow if Tr is increased. It is found that the unsteady flow is periodic for $Tr = 100$ but it turns into steady-state at $Tr = 500$ and 1000. For the rectangular duct flow of aspect ratios 2 and 3, however, time evolution calculations show that the unsteady flow is always chaotic whatever the value of Tr is. Typical contours of secondary flow patterns and axial flow distribution are obtained, and it is found that the unsteady flow is a two-, three- and four-vortex solutions for the rotating curved square duct flow, while four- to twelve-vortex solutions for the rotating curved rectangular duct flows. It is also found that the axial flow is shifted near the outer wall of the duct if Tr is increased in the positive direction.

MSC: 76Dxx • 76D99 • 76E09

Keywords: Curved duct • Secondary flow • Aspect ratio • Time-evolution • Taylor number

1. Introduction

Due to engineering applications and their intricacy, flow in a rotating curved duct has become one of the most challenging research fields of fluid mechanics. Recently, great attention has been paid for the study of flows and heat transfer through rotating curved ducts and channels because of their ample applications in chemical, mechanical, bio-mechanical and biological engineering. A quantitative analogy between flows in stationary curved pipes and orthogonally rotating straight pipes has been reported by Ishigaki [1, 2] . Taking this analogy as a basis, this study describes the characteristics of more general and complicated flow in rotating curved ducts, which are relevant to systems involving helically or spirally coiled pipes rotating about the coil axis. Such rotating flow passages are used in cooling systems in rotating machinery such as gas turbines, turbo-machinery, electric generators and electric motors. The readers are referred to Berger et al. [3] and Nandakumar and Masliyah [4] for some outstanding reviews on curved duct flows.

One of the interesting phenomena of the flow through a curved duct is the bifurcation of the flow because generally there exist many steady solutions due to channel curvature. Many researches have performed experimental and numerical investigation on developing and fully developed curved duct flows. An early complete bifurcation study of two-dimensional (2D) flow through a curved duct with square cross-section was performed by Winters [5]. However an extensive treatment of the flow through a curved square duct was performed by Mondal et al. [6]. He found a close

* Corresponding author.

E-mail address: rnmondal71@yahoo.com (Rabindra Nath Mondal)

relationship between the unsteady solutions and the bifurcation diagram of steady solutions. Ishigaki [2] examined the flow structure and friction factor numerically for both the counter-rotating and co-rotating curved circular pipe with a small curvature. Selmi et al. [7] examined the combined effects of system rotation and curvature on the bifurcation structure of two-dimensional flows in a rotating curved duct with square cross section. Selmi and Nandakumer [8] and Yamamoto et al. [9] performed the studies on the flow characteristics in rotating curved rectangular ducts. Yamamoto et al. [9] , employing the spectral method, examined the flow structure and the flow rate ratio for the flow in a rotating curved square duct and found a six-cell phenomenon of the secondary flow. Recently, Mondal et al. [10] performed comprehensive numerical study on bifurcation structure and stability of solutions for laminar forced convection in a rotating curved duct of square cross section, and revealed some new features on fluid flow.

The study of radiative heat and mass transfer in convection flow is found to be most important in industrial and technologies. The applications are often found in situation such as fiber and granules insulation, geothermal systems in the heating and cooling chamber, fossil fuel combustion, energy processes and astro-physical flows. Further, MHD flows assumes greater significance in several biological and engineering systems. The study of heat and mass transfer with chemical reaction is of particular interest to engineers and scientists due to its applications in several areas in many branches of science, engineering and technology. Bhaskar Kalita [11] performed unsteady free convection MHD flow of an incompressible viscous electrically conducting fluid under the action of transverse uniform magnetic field between two heated vertical plates by using integral transform technique. Darji and Timol [12] analyzed free convective boundary-layer problem due to the motion of an elastic surface into an electrically conducting non-Newtonian fluid. In that paper, particular attention was paid on the deductive group which provides the similarity solution of the problem. Recently, Reddy [13] analyzed the effects of first order homogeneous chemical reaction and thermal diffusion on hydro-magnetic free convection heat and mass transfer flow of viscous dissipative fluid past a semi-infinite vertical moving porous plate embedded in a porous medium in the presence of thermal radiation.

The fluid flowing in a rotating curved duct is subjected to two forces: the Coriolis force, caused by the rotation of the duct, and centrifugal force caused by the curvature of the duct. These two forces affect each other, as a result complex behavior of the secondary flow and the axial flow can be obtained (Wang and Cheng [14]). For isothermal flows of a constant property fluid, however, the Coriolis force tends to produce vorticity while centrifugal force is purely hydrostatic (Zhang et al. [15]). When a temperature induced variation of fluid density occurs for non-isothermal flows, both Coriolis and centrifugal type buoyancy forces can contribute to the generation of vorticity (Mondal et al. [16]). These two effects of rotation either enhance or counteract each other in a non-linear manner depending on the direction of wall heat flux and the flow domain. Therefore, the effect of the rotation of the system is more subtle and complicated and yields new; richer features of flow and heat transfer in general, bifurcation and stability in particular, for non-isothermal flows. Mondal et al. [16] performed numerical prediction of the non-isothermal flows through a rotating curved square duct and revealed some of such new features. They performed numerical investigation of the flows with a temperature difference between the vertical sidewalls for small Grashof number and obtained multiple branches of solutions. Very recently, Mondal et al. [17] investigated the combined effects of the Coriolis force and the centrifugal force on the flows in a rotating curved square duct numerically. The secondary flow characteristics in a curved square duct were investigated experimentally by using visualization method by Yamamoto et al. [18] . Three-dimensional incompressible viscous flow and heat transfer in a rotating U-shaped square duct were studied numerically by Nobari et al. [19]. The effects of wall curvature and rotation on the flow field and heat transfer considering different directions of rotation were presented in that paper. However, there is no known study on bifurcation and unsteady flow characteristics in a rotating curved square or rectangular duct with large rotational speed. The present paper is, therefore, an attempt to fill up this gap.

Unsteady flows by time evolution calculation of curved duct flows was first initiated by Yanase and Nishiyama [20] for a rectangular cross section. In that study, they investigated unsteady solutions for the case where dual solutions exist. However, time-dependent behavior of the flow in a curved rectangular duct over a wide range of aspect ratios was investigated, in detail, by Yanase et al. [21] numerically. They performed time-evolution calculations of the unsteady solutions with and without symmetry condition, and observed that periodic oscillations are available with symmetry condition while aperiodic time evolutions without symmetric condition. Wang and Yang [22, 23] performed numerical as well as experimental investigation on fully developed periodic oscillation in a curved square duct. Flow visualization in the range of Dean numbers from 50 to 500 was carried out in their experiment. They showed, both experimentally and numerically, that the temporal oscillation takes place between symmetric/asymmetric 2-cell and 4-cell flows where there are no stable steady flows. Applying spectral method, Yanase et al. [24] performed comprehensive numerical study of the time-dependent solutions for the non-isothermal flows through a differentially heated curved rectangular duct, and studied the effects of secondary flows on convective heat transfer. In order to study the time-dependent behavior of the unsteady solutions, recently, Mondal et al. [25] performed numerical prediction of the unsteady solutions through a stationary curved square duct flow for the isothermal flows. They showed that periodic solutions turn into chaotic solution through a multi-periodic solution, if the Dean number is increased no matter what the curvature is. However, transient behavior of the unsteady solutions, such as periodic, multi-periodic or chaotic solutions are yet unresolved for the flow through a rotating curved rectangular duct at large pressure gradient and large rotational speed. This motivated the present study to investigate the non-linear behavior of the unsteady solutions by time-evolution calculation.

In the present study, a comprehensive numerical study is presented for fully developed two-dimensional flow

of viscous incompressible fluid through rotating curved ducts of square and rectangular cross section. Studying the effects of rotation on the unsteady flow characteristics, caused by the combined action of the centrifugal and Coriolis forces, is an important objective of the present study.

2. Flow model and mathematical formulations

Consider a hydro dynamically and thermally fully developed two-dimensional flow of viscous incompressible fluid through a rotating curved duct with square and rectangular cross section. Let $2h$ and $2l$ be the height and the width of the cross section. Fig. 1 shows the coordinate system, where C is the center of the duct cross-section and L is the radius of curvature of the duct. The $x'$and y' axes are taken to be in the horizontal and vertical directions respectively, and z' is the coordinate along the center-line of the duct, i.e., the axial direction. The dimensional variables are then non-dimensionalized by using the representative length l, the representative velocity $U_0 = \frac{\upsilon}{l}$, where υ is the kinematic viscosity of the fluid. We introduce the non-dimensional variables defined as

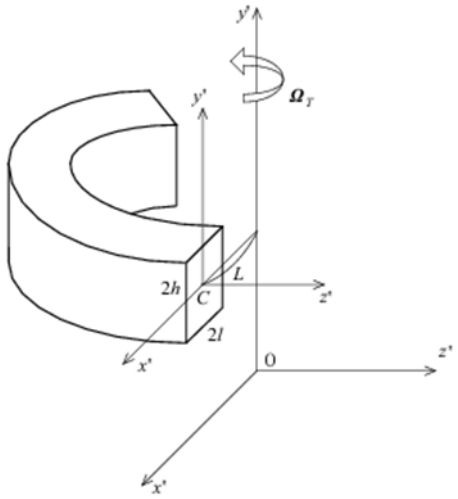

Fig. 1. Rotating coordinate system

$$u = \frac{u'}{U_0}, \quad v = \frac{v'}{U_0}, \quad w = \frac{\sqrt{2\delta}}{U_o} w', \quad x = \left(\frac{x'}{l} - \frac{1}{\delta}\right), \quad \bar{y} = \frac{y'}{l}, \quad z = \frac{z'}{l}, \quad t = \frac{U_0}{l} t', \quad \delta = \frac{l}{L}, \quad P = \frac{P'}{\rho {U_0}^2}$$

where, u, v and w are the non-dimensional velocity components in the x, $y$and z directions, respectively; t is the non-dimensional time, P is the non-dimensional pressure, δ is the non-dimensional curvature defined as $\delta = \frac{l}{L}$. Henceforth, all the variables are non-dimensionalized if not specified. Since the flow field is uniform in the z direction, the sectional stream function ψ is introduced in the s and y-directions as

$$u = \frac{1}{1+\delta x}\frac{\partial \psi}{\partial \bar{y}}, \quad v = -\frac{1}{1+\delta x}\frac{\partial \psi}{\partial x} \tag{1}$$

A new coordinate variable y is introduced in the $\bar{y}$ direction as $\bar{y} = a\, y$, where $a = \frac{h}{l}$ is the aspect ratio of the duct cross section. Then, the basic equations for w and ψ are expressed in terms of non-dimensional variables as

$$(1+\delta x)\frac{\partial w}{\partial t} + \frac{1}{a}\frac{\partial (w,\psi)}{\partial (x,y)} - Dn + \frac{\delta^2 w}{1+\delta x} = (1+\delta x)\Delta_2 w - \frac{1}{a}\frac{\delta}{(1+\delta x)}\frac{\partial \psi}{\partial y} w + \delta \frac{\partial w}{\partial x} - \delta\, Tr \frac{\partial \psi}{\partial y} \tag{2}$$

$$\left(\Delta_2 - \frac{\delta}{1+\delta x}\frac{\partial}{\partial x}\right)\frac{\partial \psi}{\partial t} = -\frac{1}{a}\frac{1}{(1+\delta x)}\frac{\partial (\Delta_2 \psi, \psi)}{\partial (x,y)} + \frac{1}{a}\frac{\delta}{(1+\delta x)^2}\left[\frac{\partial \psi}{\partial y}\left(2\Delta_2 \psi - \frac{3\delta}{1+\delta x}\frac{\partial \psi}{\partial x} + \frac{\partial^2 \psi}{\partial x^2}\right) - \frac{\partial \psi}{\partial x}\frac{\partial^2 \psi}{\partial x \partial y}\right]$$
$$+ \frac{\delta}{(1+\delta x)^2} \times \left[3\delta \frac{\partial^2 \psi}{\partial x^2} - \frac{3\delta^2}{1+\delta x}\frac{\partial \psi}{\partial x}\right] - \frac{2\delta}{1+\delta x}\frac{\partial}{\partial x}\Delta_2 \psi + w\frac{1}{a}\frac{\partial w}{\partial y} + {\Delta_2}^2 \psi + \frac{1}{2} Tr \frac{\partial w}{\partial y} \tag{3}$$

where,

$$\Delta_2 \equiv \frac{\partial^2}{\partial x^2} + \frac{1}{a^2}\frac{\partial^2}{\partial y^2}, \quad \frac{\partial (f,g)}{\partial (x,y)} \equiv \frac{\partial f}{\partial x}\frac{\partial g}{\partial y} - \frac{\partial f}{\partial y}\frac{\partial g}{\partial x} \tag{4}$$

The non-dimensional parameters Dn, the Dean number, Tr, the Taylor number which appear in Eqs. (2) and (3) are defined as:

$$Dn = \frac{Gl^3}{\mu\upsilon}\sqrt{\frac{2l}{L}}, \quad Tr = \frac{2\sqrt{2\delta}\,\Omega_T l^3}{\upsilon\delta} \tag{5}$$

where, μ is the viscosity of the fluid. In the present study, we take the curvature is constant as $\delta = 0.1$ and aspect ratio a = 1 (square duct) and $a = 2$ and 3 (rectangular duct). The rigid boundary conditions used here for w and ψ are as

$$w(\pm1, y) = w(x, \pm1) = \psi(\pm1, y) = \psi(x, \pm1) = \frac{\partial\psi}{\partial x}(\pm1, y) = \frac{\partial\psi}{\partial y}(x, \pm1) = 0 \tag{6}$$

There is a class of solutions which satisfy the following symmetry condition with respect to the horizontal plane $y = 0$.

$$\left.\begin{aligned} w(x, y, t) &\Rightarrow w(x, -y, t), \\ \psi(x, y, t) &\Rightarrow -\psi(x, -y, t), \end{aligned}\right\} \tag{7}$$

The solution which satisfies the condition (7) is called a *symmetric solution*, and that which does not an *asymmetric solution.*

3. Numerical calculations

3.1. Method of numerical calculation

In order to solve the Eqs. (2) and (3) numerically the spectral method is used. This is the method which is thought to be the best numerical method to solve the Navier-Stokes equations as well as the energy equation [Gottlieb and Orazag [26]]. By this method the variables are expanded in a series of functions consisting of the Chebyshev polynomials. That is, the expansion functions

$$\left.\begin{aligned} \varphi_n(x) &= (1 - x^2)\, C_n(x), \\ \psi_n(x) &= (1 - x^2)^2 C_n(x) \end{aligned}\right\} \tag{8}$$

where $C_n(x) = \cos(n\cos^{-1}(x))$ is the nth order Chebyshev polynomial. $w(x, y, t)$ and $\psi(x, y, t)$ are expanded in terms of $\varphi_n(x)$and $\psi_n(x)$ as

$$\left.\begin{aligned} w(x, y, t) &= \sum_{m=0}^{M}\sum_{n=0}^{N} w_{mn}(t)\,\phi_m(x)\,\phi_n(y) \\ \psi(x, y, t) &= \sum_{m=0}^{M}\sum_{n=0}^{N} \psi_{mn}(t)\,\psi_m(x)\,\psi_n(y). \end{aligned}\right\} \tag{9}$$

where, $M$and N are the truncation numbers in the x and $y$directions respectively. The expansion coefficients $w_{mn}$and ψ_{mn} are then substituted into the basic Eqs. (2) and (3) and the collocation method is applied. As a result, the nonlinear algebraic equations for$w_{mn}$and $\psi_{mn}$are obtained. The collocation points are taken to be

$$\left.\begin{aligned} x_i &= \cos\left[\pi\left(1 - \frac{i}{M+2}\right)\right], \quad i = 1, ..., M+1, \\ y_i &= \cos\left[\pi\left(1 - \frac{i}{N+2}\right)\right], \quad j = 1, ..., N+1. \end{aligned}\right\} \tag{10}$$

where $i = 1, ..., M+1$ and $j = 1, ..., N+1$. In this study, for necessary accuracy of the solutions, we use M = 20 and N = 20 for the square duct flow (aspect ratio 1) while M = 20 and N = 40 for rectangular duct flow of aspect ratio 2 and M = 20 and N = 60 for aspect ratio 3. In order to calculate the unsteady solutions, the Crank-Nicolson and Adams-Bashforth methods together with the function expansion (9) and the collocation methods are applied. Details of the method is available in Mondal et al. [6].

3.2. Resistance coefficient

The resistant coefficient λ is used as the representative quantity of the flow state. It is also called the *hydraulic resistance coefficient*, and is generally used in fluids engineering, defined as

$$\frac{P_1^* - P_2^*}{\Delta z^*} = \frac{\lambda}{dh^*}\frac{1}{2}\rho\langle w^*\rangle^2, \tag{11}$$

where, quantities with an asterisk (*) denote dimensional ones, $\langle\ \rangle$stands for the mean over the cross section of the duct and d_h^* is the hydraulic diameter. The main axial velocity $\langle w^* \rangle$ is calculated by

$$\langle w^* \rangle = \frac{v}{4\sqrt{2\delta}\, al} \int_{-1}^{1} dx \int_{-1}^{1} w\,(x, y, t)\, dy. \tag{12}$$

Since $\left(P_1^* - P_2^*\right)/\Delta_{z^*} = G$, λ is related to the mean non-dimensional axial velocity $\langle w \rangle$ as

$$\lambda = \frac{8a\sqrt{2\delta}Dn}{(1+a)\langle w \rangle^2}, \tag{13}$$

where, $\langle w \rangle = \sqrt{2\delta}\, l \langle w^* \rangle / v$. In the present study, λ is used to perform time evolution of the unsteady solutions.

4. Results and discussion

4.1. Case I: Square duct (Aspect ratio 1)

4.1.1. Time evolution of the unsteady solutions for $Tr = 100$

In order to study the non-linear behavior of the unsteady solution, we first investigate time evolution of the resistance coefficient for aspect ratio 1 (square duct). We first studied time evolution of λ for $Dn = 1000$ and $tr = 100$ as shown in Fig. 2. It is found that the flow is periodic for for $Dn = 1000$ and $tr = 100$. Typical contours of secondary flow patterns and axial flow distribution are shown in Fig. 3 for one period of oscillation. From this figure we find that secondary flow is an asymmetric two-, three-, and four-vortex solution for the periodic oscillation. Fig. 3 shows that the axial flow shifted to the outer wall of the duct where the Dean vortices are generated.

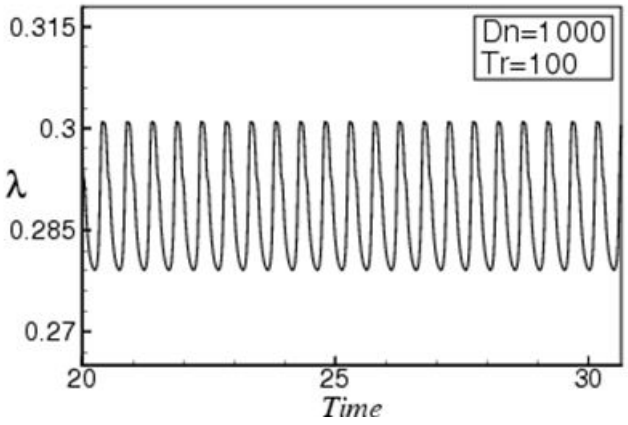

Fig. 2. Time evolution of λ for the unsteady solutions at $Dn = 1000$ and $Tr = 100$ for the aspect ratio 1 ($a = 1$)

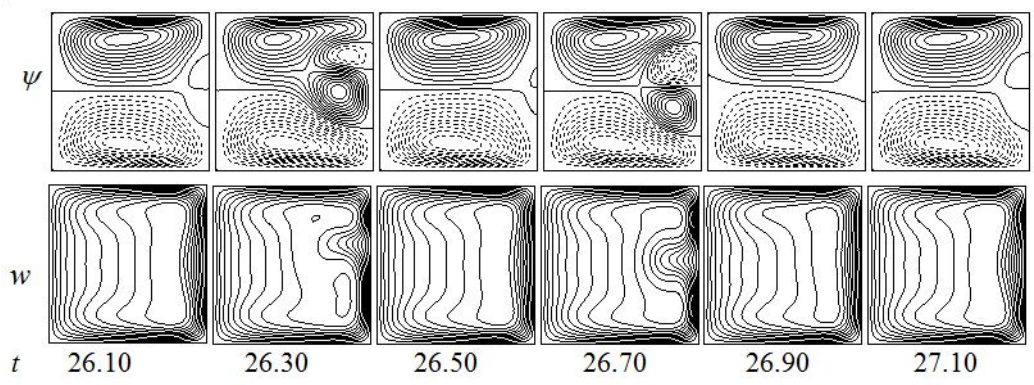

Fig. 3. Contours of secondary flow patterns (top) and axial flow distribution (bottom) for $Dn = 1000$ and $Tr = 100$ at time $26.10 \leqslant t \leqslant 27.10$

4.1.2. Time evolution of the unsteady solutions for $Tr = 500$

We studied time evolution of λ for $Dn = 1000$ and $Tr = 500$ as shown in Fig. 4(a). As seen in Fig. 4(a), the unsteady flow is a steady-state solution for $Tr = 500$. Since the flow is steady-state, we show a single contour of secondary flow pattern and axial flow distribution in Fig. 4(b). As seen in Fig. 4(b), the secondary flow is a symmetric two-vortex solution.

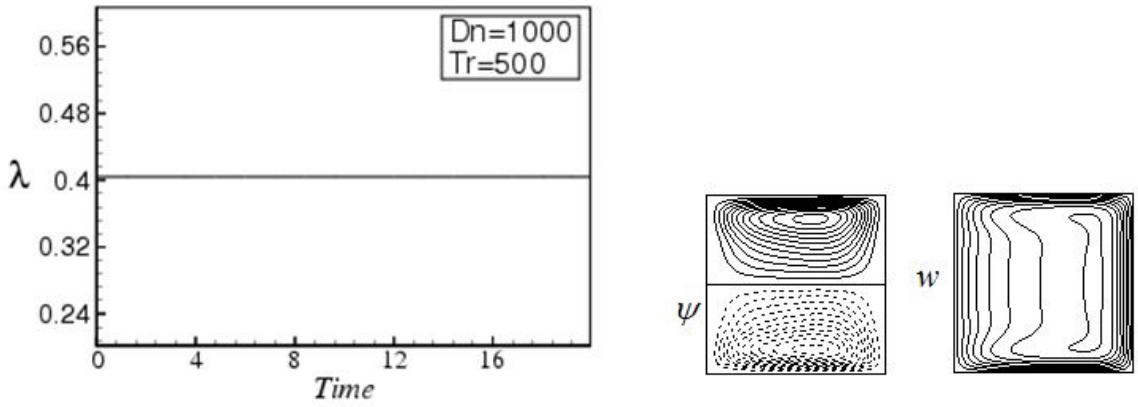

(a) (b)

Fig. 4. (a) Time evolution of λ for $Dn = 1000$ and $Tr = 500$ for the aspect ratio 1. (b) Contours of secondary flow pattern and axial flow distribution for $Dn = 1000$ and $Tr = 500$ at time $t = 16.0$

4.1.3. Time evolution of the unsteady solutions for $Tr = 1000$

We performed time evolution of λ for $Dn = 1000$ and $Tr = 1000$ as shown in Fig. 5(a). We find that the flow is also steady-state for $Tr = 1000$. Since the flow is steady-state, we show a single contour of secondary flow pattern and axial flow distribution in Fig. 5(b), where it is found that the secondary flow is also symmetric two-vortex solution.

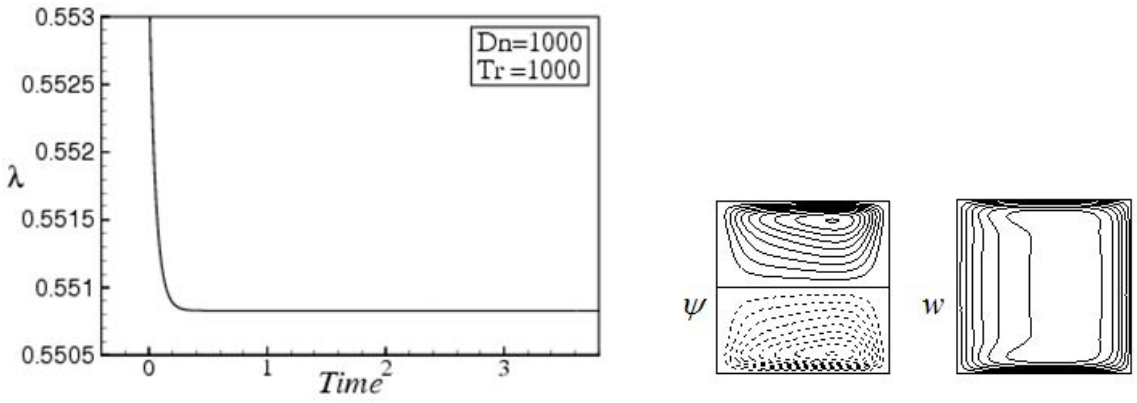

(a) (b)

Fig. 5. (a) Time evolution of λ for $Dn = 1000$ and $Tr = 1000$ for the aspect ratio 1. (b) Contours of secondary flow pattern and axial flow distribution for $Dn = 1000$ and $Tr = 1000$ at time $t = 3.0$

4.2. Case II: Rectangular duct (Aspect ratio 2)

4.2.1. Time Evolution of the unsteady solutions for $Tr = 100$

In order to study the non-linear behavior of the unsteady solution, then we investigated time evolution of λ for the curved rectangular duct of aspect ratio $a = 2$. We studied time evolution of λ for $Dn = 1000$ and $Tr = 100$ as shown in Fig. 6(a). Fig. 6(a) shows that the flow oscillates irregularly that means the flow is chaotic for $Tr = 100$. Typical contours of secondary flow patterns and axial flow distribution for $Dn = 1000$ and $Tr = 100$ are shown in Fig. 6(b) for $26.0 \leqslant t \leqslant 28.0$. As seen in Fig. 6(b), the secondary flow is four- to six-vortex solution. Fig. 6(b) also shows that the axial flow is shifted near the outer wall of the duct, and it is consistent with the secondary vortices.

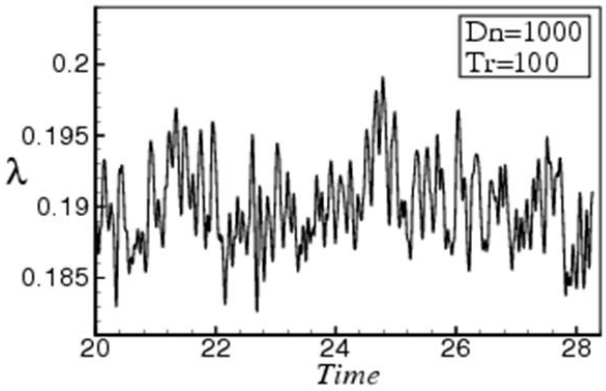

(a)

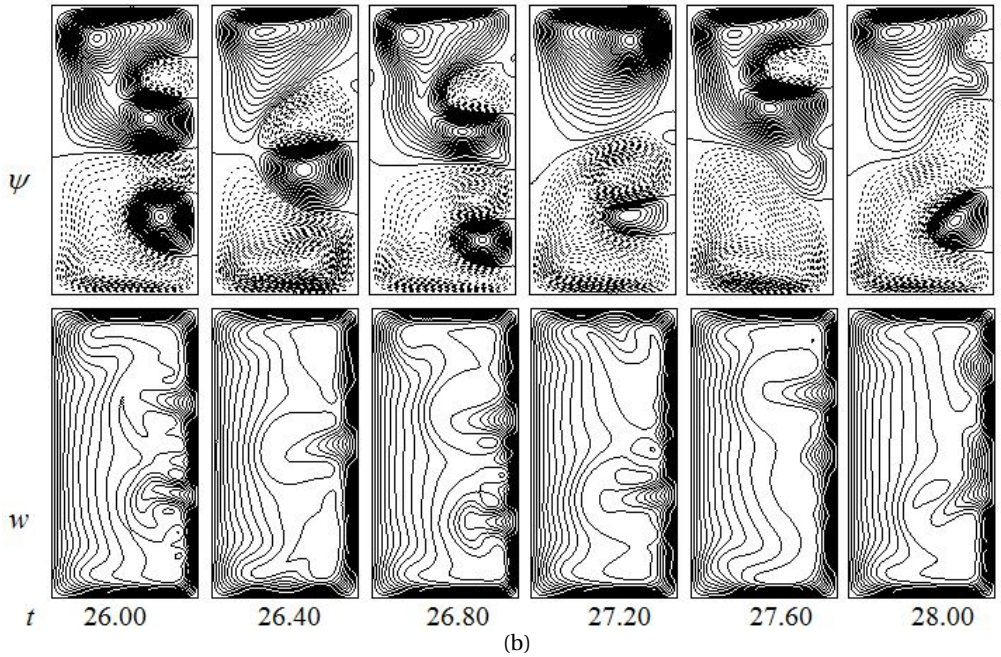

(b)

Fig. 6. (a) Time evolution of λ for $Dn = 1000$ and $Tr = 100$ for the aspect ratio 2 ($a = 2$). (b) Contours of secondary flow patterns (top) and axial flow distribution (bottom) for $Dn = 1000$ and $Tr = 100$ at time $26.0 \leqslant t \leqslant 28.0$

4.2.2. Time Evolution of the unsteady solutions for $Tr = 500$

We executed time evolution of λ for $Dn = 1000$ and $Tr = 500$ as shown in the Fig. 7(a). We find that the flow also oscillates irregularly that is the flow is chaotic for $Tr = 500$. Typical contours of secondary flow patterns and axial flow distribution for $Dn = 1000$ and $Tr = 500$ are shown in Fig. 7(b). As seen in Fig. 7(b), the secondary flow is four- to six-vortex solution for $Tr = 500$. The axial flow distribution shows that it is shifted to the outer wall of the duct and consistent with the secondary vortices as shown in Fig. 7(b).

4.2.3. Time Evolution of the unsteady solutions for $Tr = 1000$

We studied time evolution of λ for $Dn = 1000$ and $Tr = 1000$ as shown in Fig. 8(a). We find that the flow also oscillates irregularly that means it is chaotic for $Tr = 1000$. The axial flow is shifted to the outer wall and the flow is consistent with the secondary flow as shown in Fig. 8(b). Typical contours of secondary flow pattern and axial flow distribution is shown in Fig. 8(b) for $Dn = 1000$ and $Tr = 1000$. As seen in Fig. 8(b), the secondary flow is a six-vortex solution for the chaotic oscillation at $Tr = 1000$.

4.3. Case III: Rectangular duct (Aspect ratio 3)

4.3.1. Time Evolution of the unsteady solutions for $Tr = 100$

We investigated time evolution of λ for the flow through a curved rectangular duct of aspect ratio $a = 3$. Fig. 9(a) shows time evolution results for $Dn = 1000$, where we find that the unsteady flow oscillates irregularly that means the flow is chaotic for for $Dn = 1000$ and $Tr = 100$ for the aspect ratio 3. Typical contours of secondary flow patterns and

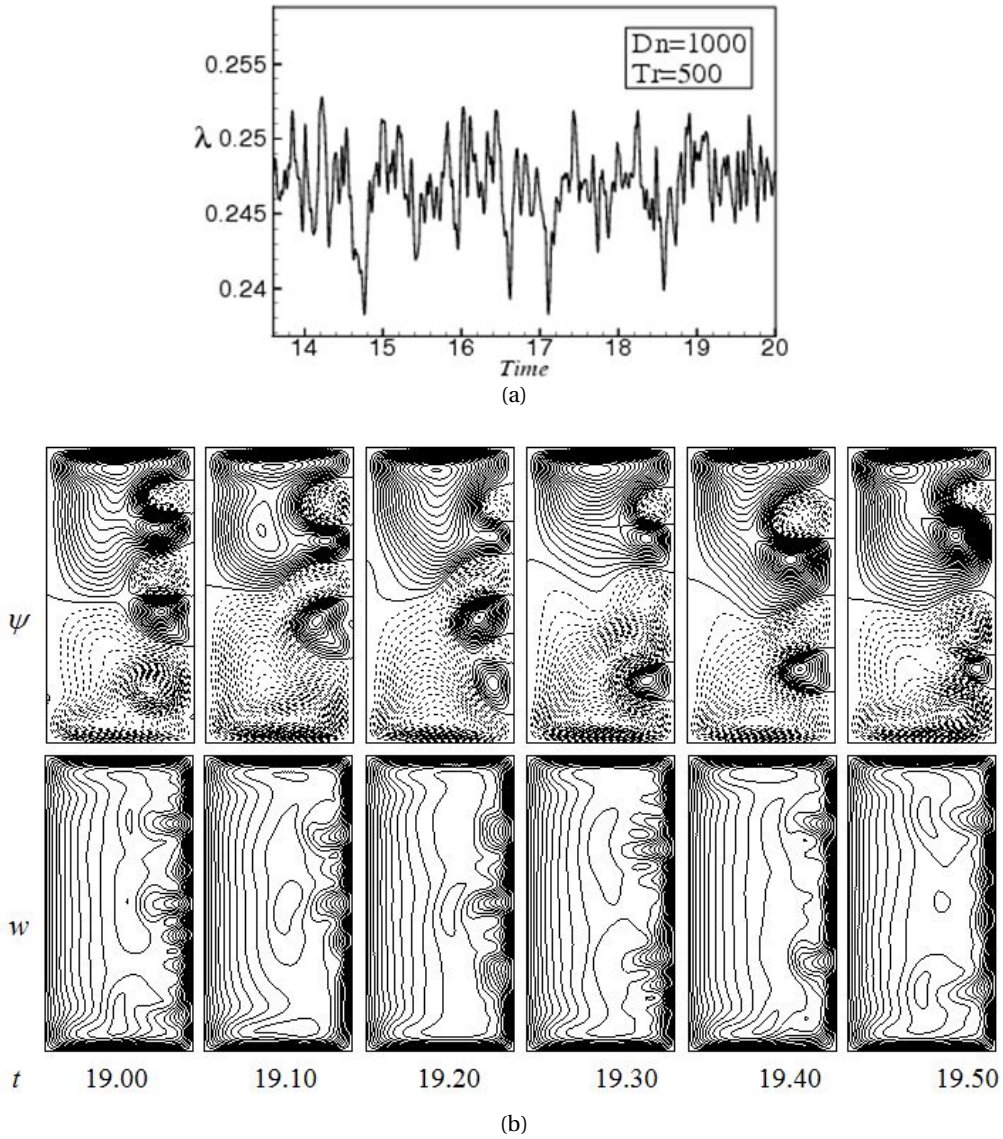

Fig. 7. (a) Time evolution of λ for $Dn = 1000$ and $Tr = 500$ for the aspect ratio 2. (b) Contours of secondary flow patterns (top) and axial flow distribution (bottom) for $Dn = 1000$ and $Tr = 500$ at time $19.0 \leqslant t \leqslant 19.50$

axial flow distribution for $Dn = 1000$ and $Tr = 100$ are shown in Fig. 9(b). As seen in Fig. 9(b), the secondary flow is an asymmetric four- to eight-vortex solution. Fig. 9(b) also shows that the axial flow is shifted near the outer wall of the duct and they are consistent with the secondary vortices.

4.3.2. Time evolution of the unsteady solutions for $Tr = 500$

We studied time evolution of λ for $Dn = 1000$ and $Tr = 500$ as shown in Fig. 10(a). Fig. 10(a) shows that the flow is chaotic for $Dn = 1000$ and $Tr = 500$. Typical contours of secondary flow patterns and axial flow distribution for $Dn = 1000$ and $Tr = 500$ are shown in Fig. 10(b) over the time interval $9.0 \leqslant t \leqslant 9.5$. As seen in Fig. 10(b), the secondary flow is an eight to twelve-vortex solution. Maximum axial flow is found to be shifted to the outer wall of the duct and the flow is consistent with the secondary flows as shown in Fig. 10(b).

4.3.3. Time evolution of the unsteady solutions for $Tr = 1000$

We performed time evolution of λ for $Dn = 1000$ and $Tr = 1000$ as shown in Fig. 11(a). We find that the flow also oscillates irregularly, that is, the flow is strongly chaotic for $Tr = 1000$. Typical contours of secondary flow patterns and axial flow distribution for $Dn = 1000$ and $Tr = 1000$ are shown in Fig. 11(b) over the time interval $34.0 \leqslant t \leqslant 35.50$. As seen in Fig. 11(b), the secondary flow is ten- to twelve-vortex solution. It is found that maximum axial flow is shifted near the outer wall of the duct as shown in Fig. 11(b). In this study, it is found that maximum number of secondary vortices is attained as the aspect ratio and the rotational speed is increased simultaneously.

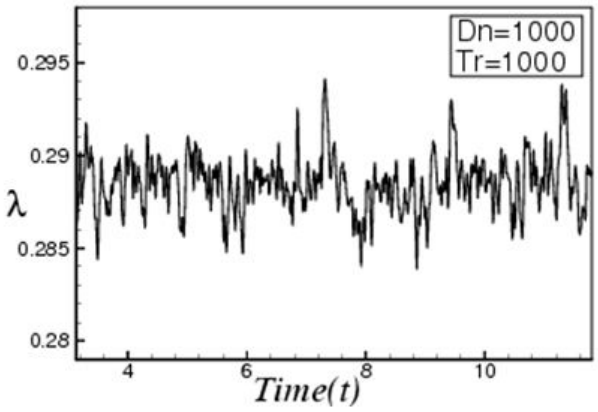

(a)

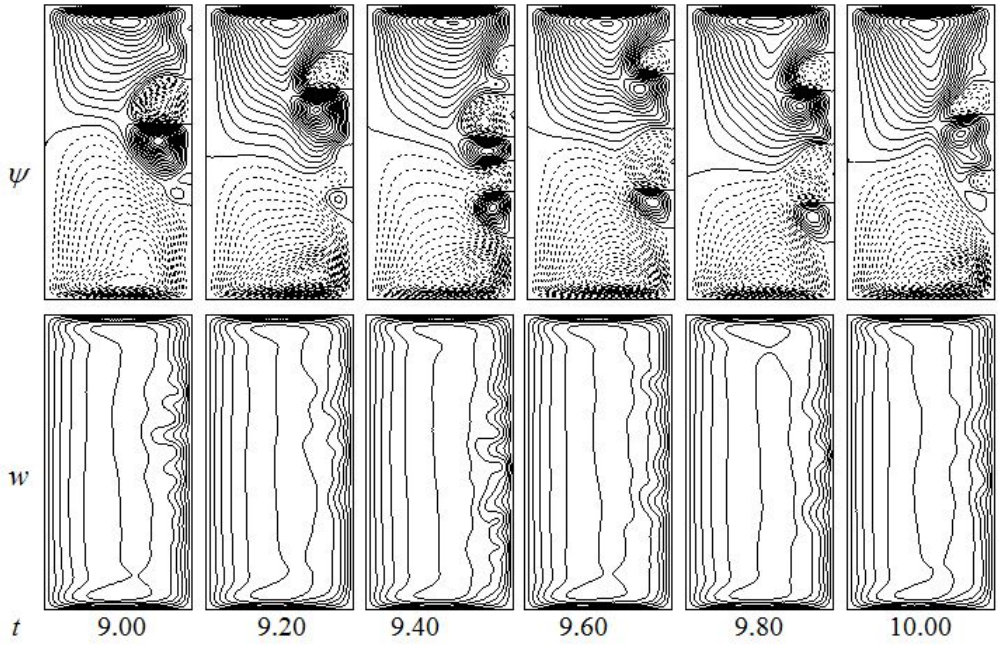

(b)

Fig. 8. (a) Time evolution of λ for $Dn = 1000$ and $Tr = 1000$ for the aspect ratio $a = 2$ (b). Contours of secondary flow patterns (top) and axial flow distribution (bottom) for $Dn = 1000$ and $Tr = 1000$ at time $9.0 \leqslant t \leqslant 10.0$

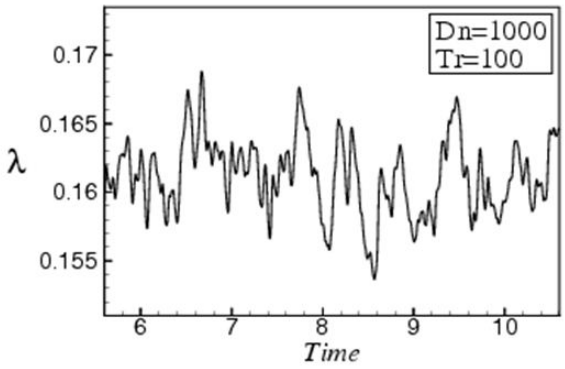

(a)

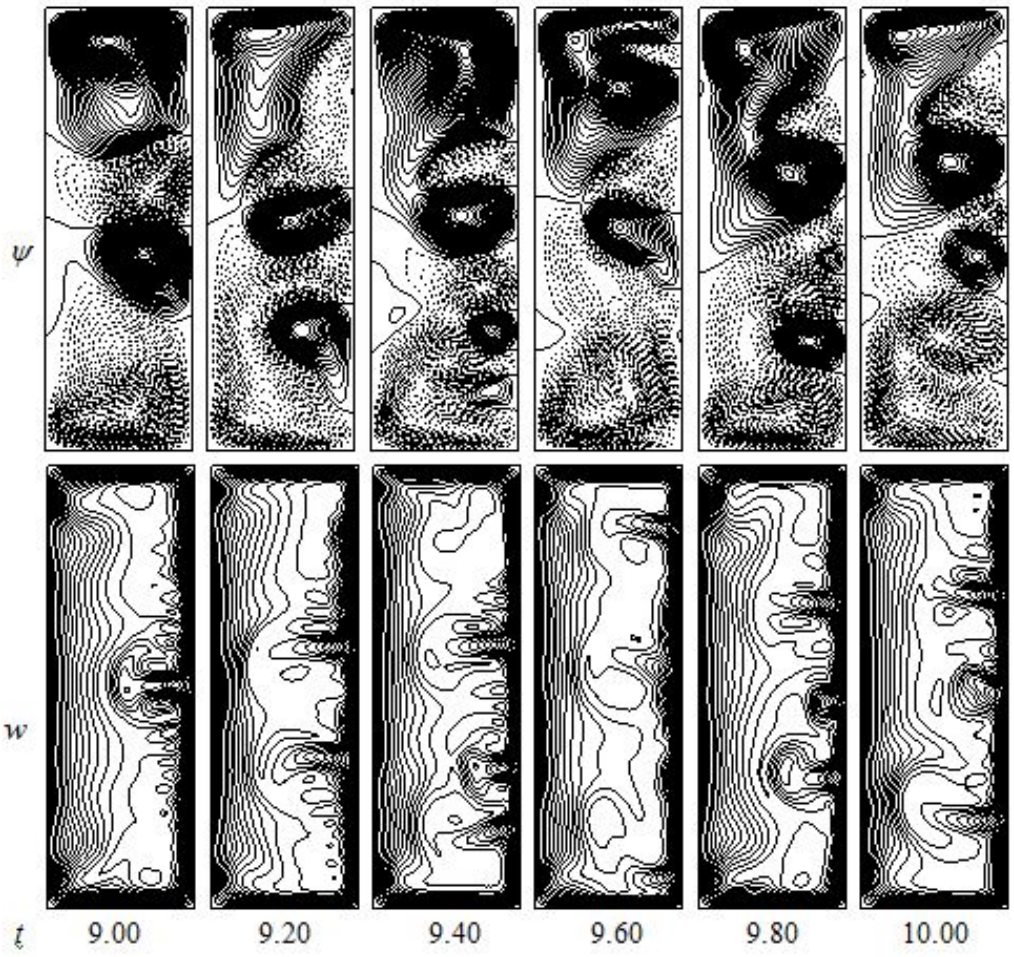

(b)

Fig. 9. (a) Time evolution of λ for $Dn = 1000$ and $Tr = 100$ for the aspect ratio 3 ($a = 3$). (b) Contours of secondary flow patterns (top) and axial flow distribution (bottom) for $Dn = 1000$ and $Tr = 100$ at time $9.0 \leqslant t \leqslant 10.0$

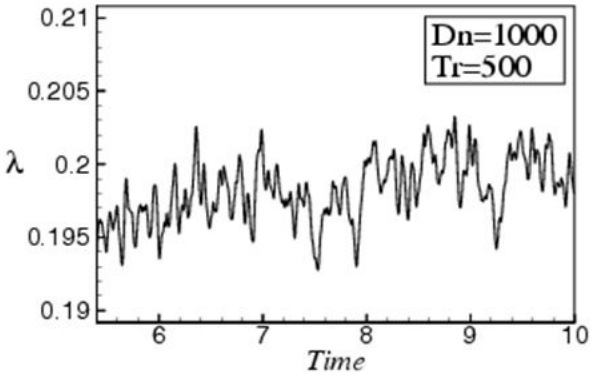

(a)

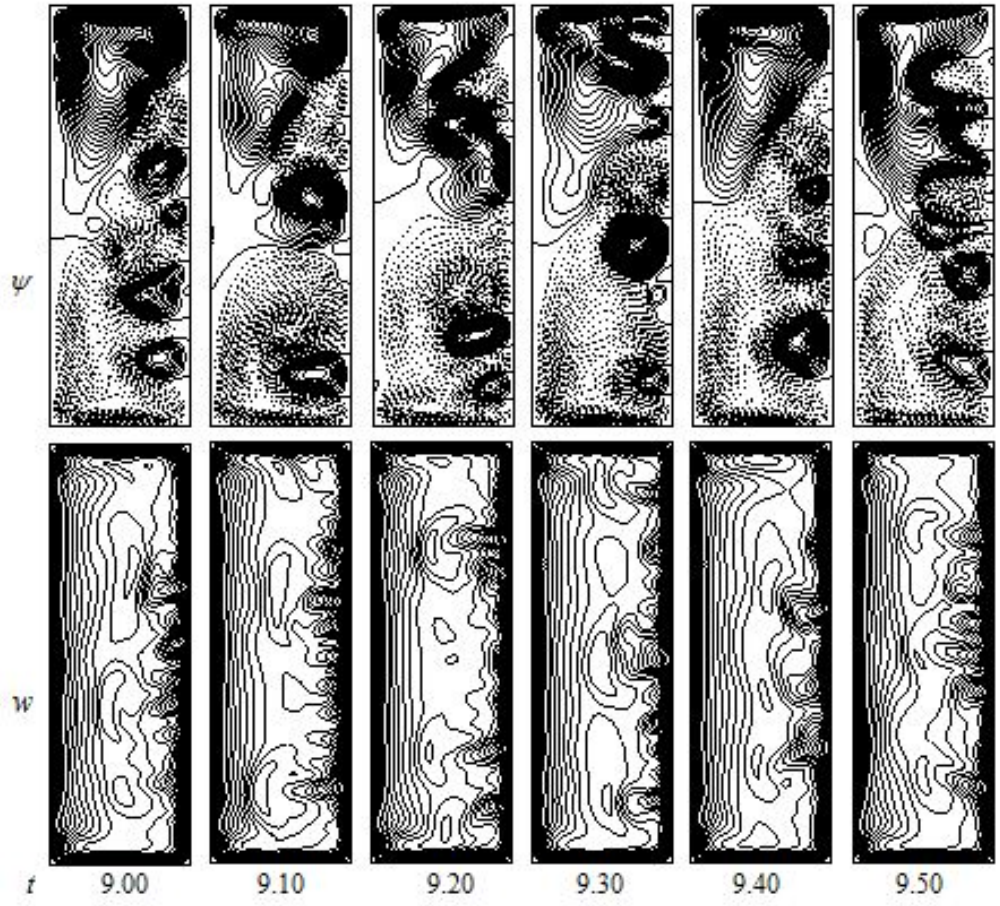

(b)

Fig. 10. (a) Time evolution of λ for $Dn = 1000$ and $Tr = 500$ for the aspect ratio 3. (b) Contours of secondary flow (top) and axial flow distribution (bottom) for $Dn = 1000$ and $Tr = 500$ at $9.0 \leqslant t \leqslant 9.5$

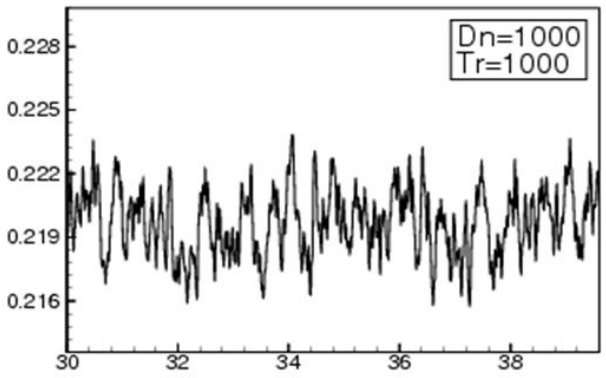

(a)

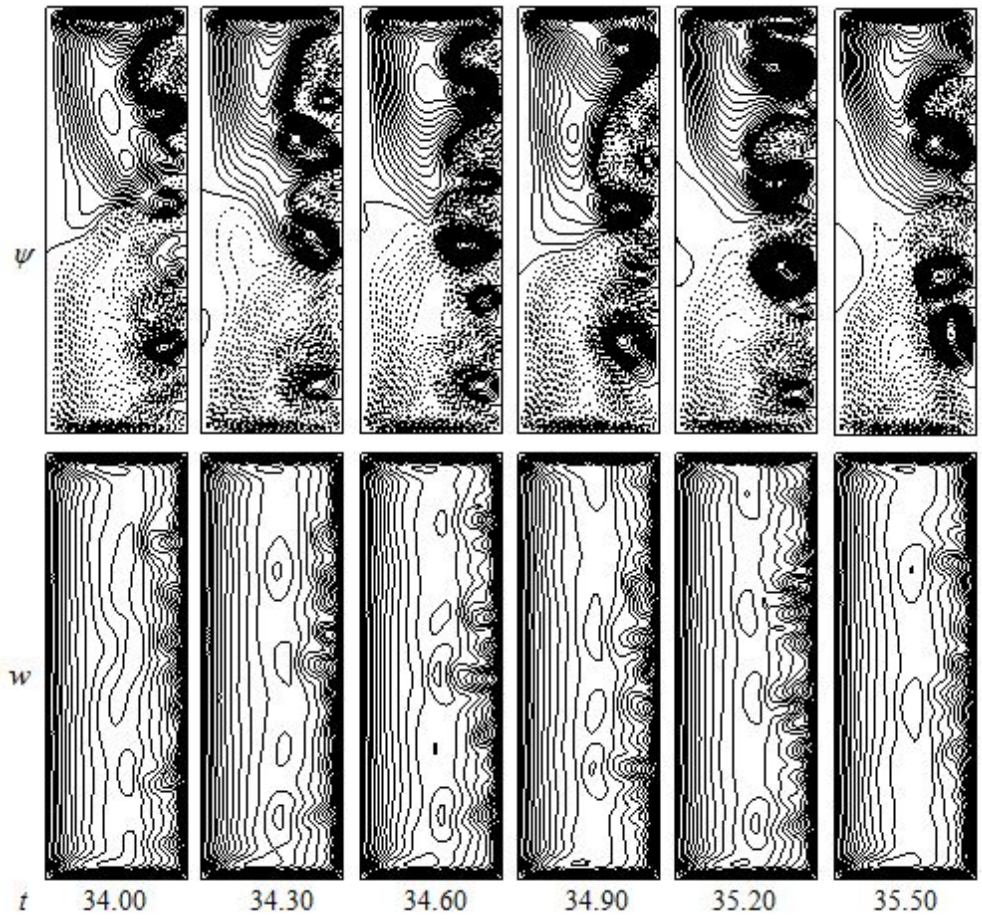

(b)

Fig. 11. (a) Time evolution of λ for $Dn = 1000$ and $Tr = 1000$ for the aspect ratio 3. (b). Secondary flow patterns (top) and axial flow distribution for $Dn = 1000$ and $Tr = 1000$

5. Conclusion

A numerical study is presented for the fully developed two-dimensional flow of viscous incompressible fluid through a rotating curved duct with square and rectangular cross sections by using a spectral method. Numerical calculations were carried out for the constant Dean number, $Dn = 1000$, over the Taylor number $Tr = 100, 500$ and 1000 for the aspect ratios 1, 2 and 3.

We investigated unsteady flow behavior and obtained contours of secondary flow patterns and axial flow distribution for such flows at several values of Tr. In order to study the non-linear behavior of the unsteady solution, we first investigated time evolution of the resistance coefficient λ for the positive rotation of the curved square duct (aspect ratio 1) and it is found that the flow is periodic for $Tr = 100$ but steady-state for $Tr = 500$ and 1000. The secondary flow is asymmetric two- and four-vortex solutions for $Tr = 100$ but symmetric two-vortex for $Tr = 500$ and 1000. Thus we see that if Tr is increased the periodic flow turns into steady-state solution. Then we investigated unsteady solutions for the curved rectangular duct flow of aspect ratio 2 and 3 for $Dn = 1000$ at $Tr = 100, 500, 1000$and it is found that the unsteady flow is a chaotic solution for any value of Tr investigated in this study. We obtained contours of secondary flow patterns and axial flow distribution for the chaotic oscillation at the above-mentioned parameters and it is found that the secondary flow is six- to eight-vortex solutions for the aspect ratio 2; however, for the aspect ratio 3, we see that the secondary flow is four- to twelve-vortex solutions. It is found that if Tr is increased the number of secondary vortices also increases at large aspect ratio. It is also found that the maximum axial flow is shifted near the outer wall of the duct as Tr is increased.

6. Acknowledgment

Rabindra Nath Mondal would gratefully acknowledge the financial support from the Japan Society for the Promotion of Science (JSPS), No. L15534, while Shinichiro Yanase expresses his cordial thanks to the Japan Ministry of Education, Culture, Sports, Science and Technology for the financial support through the Grant-in-Aid for Scientific Research, No. 24560196.

References

[1] H. Ishigaki, Fundamental characteristics of laminar flows in a rotating curved pipe, Trans. JSME 59 (1-B) (1993) 1494–1501.
[2] H. Ishigaki, Laminar flow in rotating curved pipes, Journal of Fluid Mech. 329 (1996) 373–388.
[3] S. A. Berger, L. Talbot, L. S. Yao, Flow in Curved Pipes, Annu. Rev. Fluid. Mech. 35 (1983) 461–512.
[4] K. Nandakumar, J. H. Masliyah, Swirling Flow and Heat Transfer in Coiled and Twisted Pipes, Adv. Transport Process. 4 (1986) 49–112.
[5] K. H. Winters, A Bifurcation Study of Laminar Flow in a Curved Tube of Rectangular Cross-section, Journal of Fluid Mechanics 180 (1987) 343–369.
[6] R. N. Mondal, Y. Kaga T. Hyakutake, S. Yanase, Bifurcation Diagram for Two- dimensional Steady Flow and Unsteady Solutions in a Curved Square Duct, Fluid Dynamics Research, 39 (2007) 413–446.
[7] M. Selmi, K. Namdakumar, W. H. Finlay, A bifurcation study of viscous flow through a rotating curved duct, J. Fluid Mechanics 262 (1994) 353–375.
[8] M. Selmi, K. Namdakumar, Bifurcation Study of the Flow Through rotating Curved Ducts, Physics of Fluids 11 (1999) 2030–2043.
[9] K. Yamamoto, S. Yanase, M. M. Alam, Flow through a Rotating Curved Duct with Square Cross-section, J. Phys. Soc. Japan, 68 (1999), 1173–1184.
[10] R. N. Mondal, M. R. Islam, M. S. Uddin, A. K. Datta, Flow through a Rotating Curved Square Duct: The Case of Positive Rotation, Journal of Physical Science 14 (2010) 145–163.
[11] B. Kalita, Unsteady free convection MHD flow between two heated vertical plates âĂŞ one adiabatic. Int. J. Adv. in Appl. Math. and Mech. 1(2) (2013) 146–156.
[12] R. M. Darji, M. G. Timol, Deductive group symmetry analysis for a free convective boundary-layer flow of electrically conducting non-Newtonian fluids over a vertical porous-elastic surface, Int. J. Adv. Appl. Math. and Mech. 1(1) (2013) 1–16.
[13] B. P. Reddy, MHD ïňĆow over a vertical moving porous plate with viscous dissipation by considering double diffusive convection in the presence of chemical reaction, Int. J. Adv. Appl. Math. and Mech. 2(4) (2015) 73–83.
[14] L. Q. Wang, K. C. Cheng, Flow Transitions and combined Free and Forced Convective Heat Transfer in Rotating Curved Channels: the Case of Positive Rotation, Physics of Fluids 8 (1996) 1553–1573.
[15] J. S. Zhang, B. Z. Zhang, J. Jii, Fluid flow in a rotating curved rectangular duct, Int. J. Heat and fluid flow 22 (2001) 583–592.

[16] R. N. Mondal, M. M. Alam, S. Yanase, Numerical prediction of non-isothermal flows through a rotating curved duct with square cross section, Thommasat Int. J. Sci and Tech. 12(3) (2007) 24–43.
[17] R. N. Mondal, A. K. Datta, B. Mondal, Bifurcation study of thermal Flows through a rotating curved square duct, Bangladesh Journal of Scientific and Industrial Research 48(1) (2011) 59–70.
[18] K. Yamamoto, X. Wu, K. Nozaki, Y. Hayamizu, Visualization of TaylorâĂŞDean flow in a curved duct of square cross-section, Fluid Dynamics Research 38 (2006) 1–18.
[19] M. R. H. Nobari, A. Nousha, E. Damangir, A numerical investigation of flow and heat transfer in rotating U-shaped square ducts, Int. J. Thermal Science 48 (2009) 590–601.
[20] S. Yanase, K. Nishiyama, On the bifurcation of laminar flows through a curved rectangular tube, J. Phys. Soc. Japan 57(11) (1988) 3790–3795.
[21] S. Yanase, Y. Kaga, R. Daikai, Laminar flow through a curved rectangular duct over a wide range of the aspect ratio, Fluid Dynamics Research 31 (2002) 151–183.
[22] T. Yang, L. Wang, Bifurcation and Stability of Forced Convection in Rotating Curved Ducts of Square Cross Section, Int. J. Heat Mass Transfer 46 (2003) 613–629.
[23] L. Q. Wang, T. L. Yang, Multiplicity and stability of convection in curved ducts: review and progress, Adv. Heat Transfer 38 (2004) 203âĂŞ256.
[24] S. Yanase, R. N. Mondal, Y. Kaga, Numerical Study of Non-isothermal Flow with Convective Heat Transfer in a Curved Rectangular Duct, Int. J. Thermal Sci. 44 (2005) 1047–1060.
[25] R. N. Mondal, Y. Kaga, T. Hyakutake, S. Yanase, Effects of curvature and convective heat transfer in curved square duct flows, Trans. ASME, Journal of Fluids engineering 128(9) (2006) 1013–1023.
[26] D. Gottlieb, S. A. Orazag, Numerical Analysis of Spectral Methods, Society for Industrial and Applied Mathematics, Philadelphia, USA, 1977.